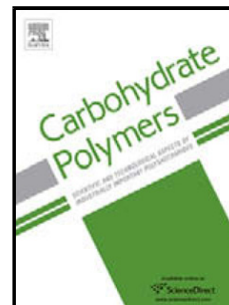


# Journal Pre-proof

Prebiotic Carbohydrates: Effect on physicochemical stability and solubility of algal oil nanoparticles

Yue Wang, Zhaojun Zheng, Kai Wang, Chuanhui Tang, Yuanfa Liu, Jinwei Li



PII: S0144-8617(19)31039-2  
DOI: <https://doi.org/10.1016/j.carbpol.2019.115372>  
Reference: CARP 115372  
To appear in: *Carbohydrate Polymers*  
Received Date: 18 June 2019  
Revised Date: 17 September 2019  
Accepted Date: 21 September 2019

Please cite this article as: Wang Y, Zheng Z, Wang K, Tang C, Liu Y, Li J, Prebiotic Carbohydrates: Effect on physicochemical stability and solubility of algal oil nanoparticles, *Carbohydrate Polymers* (2019), doi: <https://doi.org/10.1016/j.carbpol.2019.115372>

This is a PDF file of an article that has undergone enhancements after acceptance, such as the addition of a cover page and metadata, and formatting for readability, but it is not yet the definitive version of record. This version will undergo additional copyediting, typesetting and review before it is published in its final form, but we are providing this version to give early visibility of the article. Please note that, during the production process, errors may be discovered which could affect the content, and all legal disclaimers that apply to the journal pertain.

© 2019 Published by Elsevier.

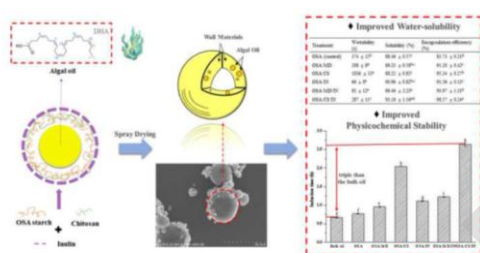
## Prebiotic Carbohydrates: Effect on physicochemical stability and solubility of algal oil nanoparticles

Yue Wang, Zhaojun Zheng, Kai Wang, Chuanhui Tang, Yuanfa Liu\*, Jinwei Li\*\*

State Key Laboratory of Food Science and Technology, Jiangnan University, Wuxi 214122, People's Republic of China

\*Corresponding Author's E-mail: [jwli@jiangnan.edu.cn](mailto:jwli@jiangnan.edu.cn) (Li, J.W.); [yfliu@jiangnan.edu.cn](mailto:yfliu@jiangnan.edu.cn) (Liu, Y.F.)

Graphical abstract



### Highlights

- Algal oil was encapsulated with 98.57% efficiency using a prebiotic system.
- Nanoparticles with OSA starch, chitosan and inulin showed high oxidative stability.
- Inulin application improved the water-solubility and wettability of the particles.

### Abstract

This study aimed at providing a novel approach for improving the physicochemical

stability and solubility of algal oil nanocapsules through formation of electrostatic interactions and prebiotic carbohydrates systems composed of: octenyl-succinic anhydride (OSA) starch, OSA/inulin (IN), OSA/maltodextrin (MD), OSA/chitosan (CS), OSA/MD/IN, and OSA/CS/IN. IN, a functional prebiotic modifier, was found to significantly ( $p < 0.05$ ) decrease emulsion viscosity and particle size, with OSA/CS/IN particles having significantly ( $p < 0.05$ ) improved water solubility (4.96%) and wettability (749 s) compared to OSA/CS particles. Interestingly, OSA/CS/IN particles had the highest oxidative stability (three times that of bulk oil) and encapsulation efficiency (98.57%). OSA/CS/IN particles were also more hygroscopic than pure OSA particles. Furthermore, scanning electron microscopy (SEM) revealed OSA/CS/IN particles had less wrinkled, smoother surfaces, providing lower air permeability and better protection. Therefore, OSA/CS/IN, as a prebiotic encapsulation system, may lead to the value addition of algal oil.

### **Abbreviations**

OSA, octenyl-succinic anhydride; IN, inulin; MD, maltodextrin; CS, chitosan; EE, encapsulation efficiency; IT, induction time; UGO, universal global optimization method; FTIR, Fourier transform infrared spectroscopy; TGA, Thermogravimetric analysis; dTG, derivative thermogravimetry;  $a_w$ , water activity.

**Keywords:** Carbohydrates, prebiotic, algal oil, physicochemical stability, solubility

### **1. Introduction**

Algal oil is rich in omega-3 polyunsaturated fatty acids (PUFA), specifically

docosahexaenoic acid, which has been associated with reduced inflammation and prevention of cardiovascular disease and infant dysplasia (Sun-Waterhouse, 2011; Ortea, Gonzalez-Fernandez, Ramos-Bueno, & Guerrero, 2018; and Che, Li, Zhang, Wang, & Wang, 2018). Unfortunately, incorporation of algal oil into foods has several obstacles, including high oxygen sensitivity and low water solubility, which limit its applications in food formulation (Akhavan, Assadpour, Katouzian, & Jafari, 2018). Recently, microencapsulation technology has been advocated as an approach to improve lipid solubility and prevent oxidation of omega-3 PUFA oils, such as algal oil (Encina, Vergara, Giménez, Oyarzún-Ampuero, & Robert, 2016). Maintaining physical, chemical, and biological properties is the primary goal of microencapsulation processes. The characteristics of algal oil can be enhanced by encapsulating it as nanoparticles with functional coatings.

It is well acknowledged that the selection of the wall material plays an important role in the microencapsulation process, as its physical properties are supposed to improve the physicochemical characteristics of the encapsulated substances (Garcia, Tonon, & Hubinger, 2012). Octenyl succinic anhydride starch (OSA starch), a typical modified polysaccharide that is both amphipathic and non-toxic, is an excellent emulsifier and has a high oil-load capability for spray drying. By the other side, it does have some deficits in terms of solubility and stability, as no single encapsulation material is capable of offering complete diversity of characteristics (Frascareli, Silva, Tonon, & Hubinger, 2012). By combining various polysaccharides, this deficit can be improved. For instance, the addition of xanthan gum and arabic gum to OSA starch has

been shown to enhance the oxidative stability and solubility of microcapsules (He et al., 2016; and Fernandes, Borges, & Botrel, 2014). Maltodextrin (MD), a popular polysaccharide with high water solubility, can also improve particle properties. When used in combination with OSA starch, MD poor emulsification properties can be overcome (Otalora, Carriazo, Iturriaga, Nazareno, & Osorio, 2015; and Bule, Singhal, & Kennedy, 2010). Particularly, another polysaccharide, chitosan (CS), has protonated amino groups which can associate with the carboxylic groups of OSA starch. The electrostatic complexes formed confer enhanced stability to capsules and stabilize their sensitive cores against oxidation (Utai, Pairat, Pavinee, D Julian, & Decker, 2005).

In addition to these characteristics, currently, because of growing consumer interest in “functional foods”, prebiotic coating materials are being emphasized for their benefits. Inulin (IN), a prebiotic polysaccharide consisting of fructose units linked by  $\beta$ -(2, 1) bonds with a 10 to 60 degree of polymerization, is at the forefront of the emerging trend toward functional characteristics and low caloric value. A few studies have demonstrated that prebiotics, such as IN, can be used as modifiers in the formulation of foods for its excellent water-solubility and surface activity (Cho & Samuel, 2009; and Silva, Zabet, Cazarin, Jr, & Meireles, 2016). In this regard, the new encapsulation systems containing IN can promote the application possibilities of the algal oil.

To our knowledge, there is limited information exploring the new approach to improve the physicochemical stability and solubility of algal oil nanoparticles. Therefore, this work investigated prebiotic carbohydrate systems and their effects on

the physicochemical characteristics of nanocapsules containing high algal oil contents. By measuring rheological parameters, water solubility, particle size, and encapsulation efficiency, the basic physicochemical indexes were obtained. Additionally, through use of the Rancimat method, moisture adsorption isotherms, and thermogravimetric analysis (TGA) particle stability was evaluated.

## **2. Materials and method**

### **2.1. Materials**

Algal oil was obtained from Huison Biotech Co., Ltd. (Xiamen, China). The following compounds were used as wall materials: OSA starch (Capsul®, National Starch Food Innovation, São Paulo, Brazil), MD with 15 DE (Sigma–Aldrich, Shanghai, China), water-soluble CS (Yuanye Biotech Ltd., Shanghai, China) and IN (91% inulin) with a degree of polymerization of 10 (Siba Ingredients, São Paulo, Brazil). The oil had a composition of 50% docosahexaenoic acid (C22:6) and no antioxidants were added, in accordance with the supplier. All other chemicals and solvents used were of analytical grade.

### **2.2. Experimental design**

All measurements were conducted in duplicate, using 5:1 ratios of OSA: other wall material (MD+CS+IN), as shown in **Table 1**, optimized in previous work.

**Table 1.** Experimental design of the components in emulsion formulations.

Components	Ratio	Wall Material (g/100g emulsion)				Core Material (g/100g emulsion)
		OSA	MD	CS	IN	Algal oil
OSA (control)	—	25.00	—	—	—	10.00
OSA/MD	5:1	20.84	4.16	—	—	10.00
OSA/CS	5:1	20.84	—	4.16	—	10.00
OSA/IN	5:1	20.84	—	—	4.16	10.00
OSA/MD/IN	5:0.5:0.5	20.84	2.08	2.08	—	10.00
OSA/CS/IN	5:0.5:0.5	20.84	—	2.08	2.08	10.00

OSA (OSA starch), MD (maltodextrin), CS (chitosan), IN (inulin).

### 2.3. Preparation and spray drying of algal emulsions

Aqueous solutions of each emulsion were prepared by dissolving wall materials (25%, w/w) in distilled water under magnetic stirring at 700 rpm at room temperature overnight for complete hydration (Carvalho, Silva, & Hubinger, 2014). The algal oil (10% w/w) was added gradually to the aqueous solution under 13,000 rpm stirring for 10 min using a rotor-stator mixer (T 18 basic ULTRA-TURRAX, IKA, Wilmington, USA). After homogenization by mechanical agitation, the emulsions were ultrasonicated (Digital Sonifier, JY92-IIN, Ningbo Scientz Biotechnology Co., Ltd., Ningbo, Zhejiang, China) for 20 min to ensure complete emulsification. The digital sonifier (800 W) was equipped with a cylindrical titanium sonotrode probe with a diameter of 60 mm. The ratio of the wall material to algal oil was maintained at 2.5:1 (w/w).

After preparation, the emulsions were immediately subjected to a spray dryer (SD-1500, Triowin, Shanghai, China) using a flexible tube pump. The parameters used: inlet air temperature  $175 \pm 5^\circ\text{C}$  and outlet air temperature  $75 \pm 5^\circ\text{C}$ , were previously

established by He et al., (2016). The feed flow and drying air flow rates were maintained at 0.6 L/h and 35 L/min, respectively.

#### **2.4. Rheological parameters of emulsions**

The rheological properties of the algal oil emulsions and the wall material aqueous solutions were measured as described by Botrel, de Barros Fernandes, Borges, and Yoshida (2014). The rheological experiments were conducted using a rheometer (TA, Discovery Series Hybrid DHR-3, USA) at 25 °C with a cone plate configuration (60 mm diameter, 2°), and flow curves were obtained at shear rates of 0.1–200 s<sup>-1</sup>.

#### **2.5. Particle morphology**

OSA, OSA/MD/IN, and OSA/CS/IN nanoparticles were deposited on carbon double-sided adhesive tape, mounted on stubs, and sputtered with gold under vacuum prior to examination by a scanning electron microscope (SU 1510, Hitachi, Tokyo, Japan). The voltage was conducted at 20 kV with 1200× and 900× magnification times.

#### **2.6. Particle size distribution**

The algal oil particle size distributions were measured using a particle size analyzer (NanoBrook Omni, Brookhaven Instruments Corp., NY, USA). Samples were prepared by dispersing 0.9 g of each sample in 150 mL of distilled water under magnetic stirring. The particle size distributions were then monitored until constant readings were obtained. Using the Stokes-Einstein equation, the effective (hydrodynamic) diameters of the particles were calculated, and the mean diameters were calculated as the average of the effective diameters (sum divided by number of runs). Based on the scattering intensities of the different sized particles, intensity distributions were also measured

(Wang, Jiang, & Xiong, 2018).

## 2.7. Moisture content of algal oil particles

The moisture contents of the particles were measured using the AOAC method. Samples were dried at 105 °C until constant weight, and their moisture contents (%) were calculated based on their mass loss.

## 2.8. Water solubility and wettability of algal oil particles

Cold water solubility of the particles was determined according to a method reported by Cano-Chauca, Stringheta, Ramos, and Cal-Vidal (2005) with some modifications. Weighed powder samples (500 mg) were dissolved in distilled water (12 mL) and stirred at a low speed (200 rpm) for 15 s. After all of the particles were added, the mixture was transferred to high speed (1500 rpm) for 2 min. The emulsions were then centrifuged at 1500rpm for 20 min, and a 4 mL aliquot of the supernatant was transferred from centrifuge tube to a Petri dish and dried at 100 ° C for 4 h. Based on Eq. (1), the cold-water solubility (S) is obtained:

$$S(\%) = \frac{\text{grams of solids in supernatant} \times 3}{\text{grams of powder}} \times 100\% \quad (1)$$

Wettability of the particles was measured according to the study of Fuchs et al. (2006) with a few adaptations. The particle samples (0.1 g) were spread on the surface of distilled water (100 mL) at 20°C without stirring. The amount of time it took for the last powder particles of each sample to submerge was recorded and used to compare the wettability of each treatment.

## 2.9. Surface oil content and encapsulation efficiency of algal oil particles

The amount of surface oil was based on a method of petroleum ether extraction (García, Gutiérrez, Nolasco, Carreón, & Arjona, 2006) and conducted according to the study of Botrel et al. (2014). The surface oil content of each powder was used as an indication of its encapsulation efficiency. In this study, total oil was calculated as the initial oil added because algal oil is non-volatile. Besides, it is considered that degradation of the oil at high temperature attached to the dryer wall are ignorable (Jafari, Assadpoor, He, & Bhandari, 2008). The encapsulation efficiency (EE) was calculated using **Eq. (2)**:

$$EE(\%) = \frac{\text{Total oil} - \text{surface oil}}{\text{Total oil}} \times 100\% \quad (2)$$

## **2.10. Fourier transform infrared spectroscopy of algal oil particles**

The FTIR spectra of the treatments were measured using a spectrometer (Thermo Scientific, Nicolet iS10, MA, USA) at room temperature, in the range of 400-4000  $\text{cm}^{-1}$ . Moreover, spectra were averaged over 40 scans and were measured with a 2  $\text{cm}^{-1}$  resolution ratio.

## **2.11. Lipid oxidation of algal oil particles**

The oxidation stability of the powders was assessed using the Rancimat method, in which the volatile oxidation products of the samples are monitored based on the induction time (IT). IT is considered as the time spent (h) to reach the inflection point of the curve ( $K = f(t)$ ), obtained from the intersection of the line tangent to the curve projected along the time axis. Accelerated measurements of the powders and pure algal oil were performed in duplicate, using a Rancimat apparatus (892, Metrohm AG,

Herisau, Switzerland), with 0.5 g of each powder heated to 120 °C under a constant bubbling airflow of 20 L/h (Giorgio, Salgado, & Mauri, 2019).

### 2.12. Moisture adsorption isotherm of algal oil particles

According to the results of wettability, solubility, efficiency encapsulation and oxidative stability of algal oil particles, OSA/MD/IN and OSA/CS/IN were chosen to analysis the sorption isotherms using the static gravimetric measurement with a series of saturated saline solution at 25°C. The OSA was used as a control group. Eight saturated saline solutions (LiCl, CH<sub>3</sub>COOK, MgCl<sub>2</sub>, K<sub>2</sub>CO<sub>3</sub>, CuCl<sub>2</sub>, NaCl, KCl, and K<sub>2</sub>SO<sub>4</sub>) were applied to satisfy the water activity range 0.11-0.98. The GAB, BET, Halsey, Henderson, Oswin, and Smith mathematical models were used to correlate moisture adsorption isotherm data with water activity. The association between mathematical models and experimental data was found, along with the estimated parameters of these equations, using a universal global optimization (UGO) algorithm of 1stOpt 5.0 software. The most suitable model was defined as possessing the lowest relative mean error (E) and highest adjusted R-squared (Adj. R<sup>2</sup>) values (Botrel & Souza, 2016), which was calculated using **Eq. (3)**:

$$E = \frac{100}{N} \sum_{i=1}^N \frac{|m_{ei} - m_{pi}|}{m_{ei}} \quad (3)$$

where  $m_{ei}$  is the experimental value,  $m_{pi}$  is the predicted value, and  $N$  is the number of the experimental data.

### 2.13. Thermogravimetric analysis (TGA) of algal oil particles

A thermobalance (Mettler Toledo, TGA2, Zurich, Switzerland) was used to obtain

derivative thermogravimetry (dTG) curves of the samples; the operating conditions were as follows: dynamic nitrogen atmosphere with a rate of 20 mL/min; temperature range: 50–500°C; heating rate: 10°C/min.

#### 2.14. Statistical Analysis

Analysis of variance ANOVA was conducted to assess the effect of six different wall material systems on the parameters studied. The differences in the mean values obtained were examined by the Duncan means test at  $P < 0.05$  significance level. All statistical analysis was performed utilizing the software SPSS (version 19.0).

### 3. Results and discussion

#### 3.1. Rheological parameters of emulsions

The flow behavior index ( $n$ ) is a measurement of how similar an emulsion is to Newtonian fluid. OSA, OSA/MD, OSA/IN, OSA/MD/IN algal oil emulsions presented trends of Newtonian fluids ( $n=1$ ), as shown in **Table 2**. Interestingly, the  $n$  value of OSA/CS/IN, OSA/CS emulsions were lower, which were defined as pseudoplastic fluids ( $n < 1$ ). The similar result was also obtained by Hwang and Shin (2000), and they observed that elastic properties increased with increasing CS concentration. These results may be attributed to higher alignment of the molecules towards the formed flows inducing higher fluidity of the liquid, as suggested by Nsofor and Osuji (1997). Additionally, the type of encapsulation system significantly ( $p < 0.05$ ) influenced the variations observed in the consistency coefficient values, with the highest value seen for the OSA/CS emulsion, indicating its high viscosity. According to **Figure 1**, the

OSA/CS emulsion presented the highest viscosity value because of its electrostatic interactions between the protonated amino groups of CS and the carboxylic groups of the OSA starch. However, the viscosity of the OSA/CS/IN emulsion was significantly ( $p < 0.05$ ) lower than that of the OSA/CS sample; this was because the addition of IN reducing the proportion of CS in the system, leading to a reduction in electrostatic interactions. Additionally, IN, being a short-chained fructooligosaccharide having a degree of polymerization of 10, is a soluble fiber, having a viscosity similar to that of water (Mensink, Frijlink, Maarschalk, & Hinrichs, 2015). Likewise, OSA/MD/IN showed a lower viscosity value compared to that of OSA/MD. Intriguingly, Jafari, Assadpoor, Bhandari, et al. (2008) found that the encapsulation efficiency was influenced by the emulsion viscosity to a certain extent, because the high viscosity increases the surface oil content owing to slower droplet formation and the longer exposure in the process of spray drying.

**Table 2.** Rheological parameters, statistical parameters for the emulsions and particle size distribution parameters for the nanoparticles produced with the different wall material systems.

Treatments	Rheological parameters (emulsions)		Statistical parameters		Particle size distribution parameters (nanoparticles)	
	Consistency coefficient, K (mPa•s <sup>n</sup> )	Flow behavior index, n	R <sup>2</sup>	E (%)	Mean diameter (nm)	PDI
OSA (control)	24.2 ± 0.1 <sup>c</sup>	1.000 ± 0.000 <sup>a</sup>	1.000000	1.16	388.74 ± 6.21 <sup>b</sup>	0.18
OSA/MD	24.0 ± 0.3 <sup>c</sup>	0.994 ± 0.001 <sup>a</sup>	0.999998	1.90	361.63 ± 8.04 <sup>c</sup>	0.16
OSA/CS	119.4 ± 1.6 <sup>a</sup>	0.974 ± 0.001 <sup>c</sup>	0.999992	4.10	644.46 ± 3.74 <sup>a</sup>	0.11
OSA/IN	16.6 ± 0.1 <sup>e</sup>	0.992 ± 0.003 <sup>a</sup>	0.999998	2.22	223.70 ± 2.08 <sup>e</sup>	0.19
OSA/MD/IN	19.4 ± 0.3 <sup>d</sup>	1.001 ± 0.000 <sup>a</sup>	0.999999	0.76	305.58 ± 2.70 <sup>d</sup>	0.15
OSA/CS/IN	29.3 ± 0.6 <sup>b</sup>	0.982 ± 0.004 <sup>b</sup>	0.999998	2.96	394.67 ± 1.48 <sup>b</sup>	0.17

<sup>a,b,c,d,e</sup> Values with different letters at the same column differ significantly ( $p < 0.05$ ) by Duncan test; E

(relative mean error); PDI (polydispersity index); Mean diameter was the average of effective (hydrodynamic) diameters (sum divided by number of runs); OSA (OSA starch), MD (maltodextrin), CS (chitosan), IN (inulin).

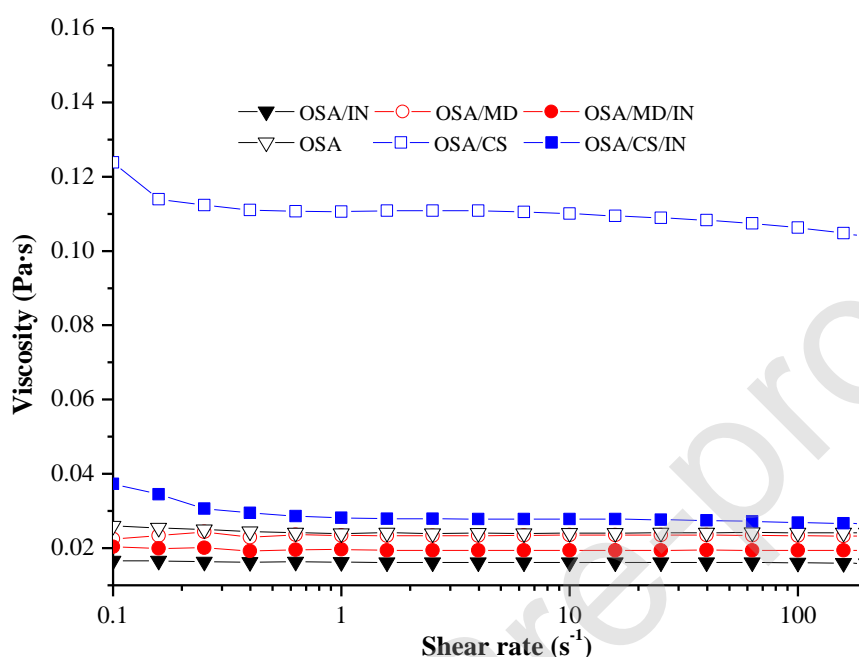


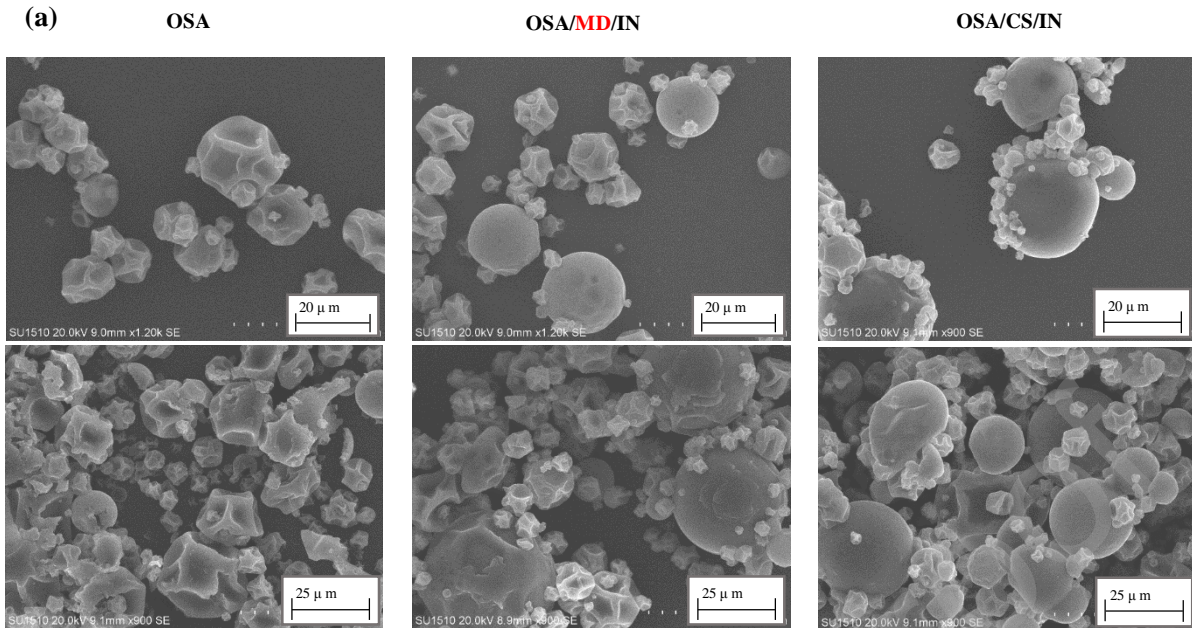
**Figure 1.** Emulsions viscosity as a function of shear rate. OSA (OSA starch), MD (maltodextrin), CS (chitosan), IN (inulin).

### 3.2. Particle morphology

Particle morphology plays a vital role in the study of omega-3 oil encapsulation as their surface characteristics can influence physicochemical properties. The morphological characterization of OSA, OSA/MD/IN and OSA/CS/IN nanoparticles (**Figure 2a**) presented the surfaces with no fissures or cracks, which were necessary to guarantee low air permeability and better protective effect. Nevertheless, variations in the wrinkles of the powder surfaces were emerged. These wrinkles, according to

Carneiro, Tonon, Grosso, and Hubinger (2013) are the results of an uneven film formation at the start of the drying process of the small droplets. Surfaces of the particles produced using OSA/MD/IN and OSA/CS/IN had fewer wrinkles as compared to those produced using pure OSA, this was most likely because of the higher molecular flexibility of a mixture of these carbohydrates, which showed massive possible conformations (Lacerda et al., 2016). Furthermore, particles produced using OSA/CS/IN showed a smoother surface than OSA/MD/IN, which maybe because of the formation of an electrostatic force between the CS and the OSA starch (Klinkesorn, Decke, & McClements, 2006). It leads to an increased interaction between wall materials, thereby hindering shrinkage.

Additionally, the particles showed varying degrees of agglomerations, which were in agreement with a reported by Hategekimana, Masamba, Ma, and Zhong (2015), who studied vitamin E nanoparticles produced using several types of OSA starches systems. The level of agglomeration was higher for OSA/CS/IN treatments, followed by OSA/MD/IN treatments; the pure OSA treatment was the lowest. These observations results were mainly attributed to the hygroscopic nature of the wall materials, which was verified by the moisture adsorption isotherm, as will be seen later.



(b)

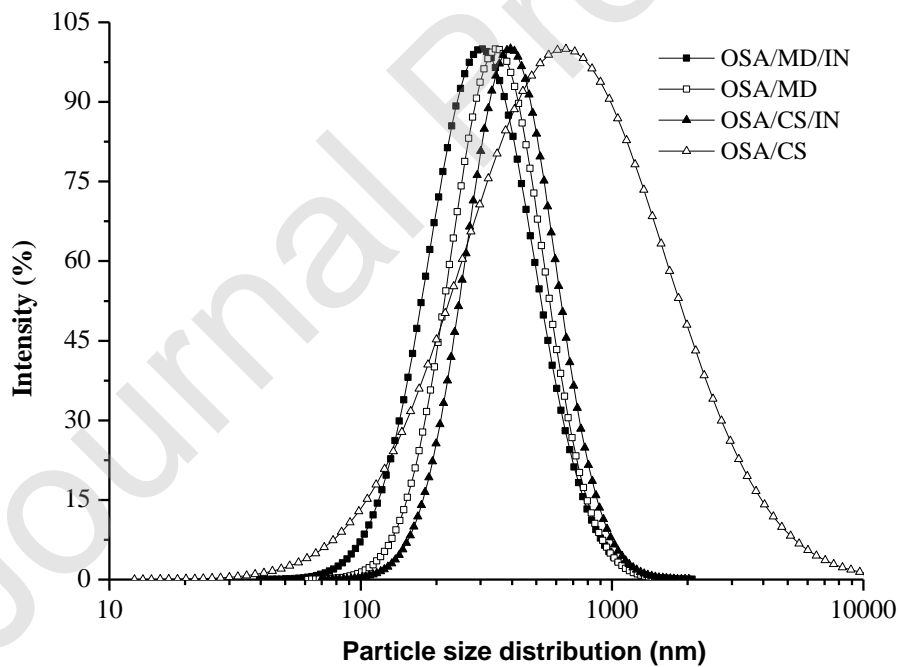


**Figure 2.** Scanning electron micrographs of the nanoparticles (a). Particle size distribution of the nanoparticles produced using the different wall material systems studied (b). OSA (OSA starch), MD (maltodextrin), CS (chitosan), IN (inulin).

### 3.3. Particle size distribution

The mean diameters of the nanoparticles were 644.46 nm, 394.67 nm, 388.74 nm, 361.63 nm, 305.58 nm, and 223.70 nm for the OSA/CS, OSA/CS/IN, OSA, OSA/MD, OSA/MD/IN and OSA/IN treatments, respectively (**Table 2**). The particle distribution was considered homogeneous based on PDI values (0.11–0.19). According to Mirhosseini, Tan, Hamid, and Yusof (2008), a polydispersity index less than 0.3 is normally defined as a narrow distribution in spray drying.

The type of wall matrix systems significantly affected ( $p < 0.05$ ) the particle size. Algal oil nanoparticles encapsulated with OSA/MD/IN (compared with OSA/MD) and OSA/CS/IN (compared to OSA/CS) showed lower particle size value and narrower distribution in **Figure 2b**. According to a study by Reineccius (2004), more viscous emulsions form larger droplets during atomization and produce larger sized particles. Hence, the particles having smaller mean sizes and narrower distributions in the presence of IN could be attributed to the ability of this carbohydrate to form solutions with low viscosities. Furthermore, these results were in agreement with findings by Botrel et al. (2014).

### 3.4. Particles characterization

The average and standard deviation values of the moisture content, wettability, solubility and surface oil content of the OSA, OSA/MD/IN, OSA/MD, OSA/CS/IN, OSA/CS and OSA/IN nanoparticles are shown in **Table 3**. These properties influence the particle behavior during the processing, sales, and storage of the final product

(Cristian Dima, Pătrașcu, Cantaragiu, Alexe, & Dima, 2015).

The particles produced using IN differed statistically ( $p < 0.05$ ) from the others in terms of moisture content, with the powders encapsulated using OSA/MD, OSA/CS, and pure OSA having the highest moisture contents. The differences in the moisture content presented between particles were due to the affinities of the materials to water and moisture diffusivities through the wall matrix (Botrel et al., 2017). It was observed that the inclusion of IN facilitated the moisture reduction of the particles, which was supported by the study of Botrel and Souza (2016). For the particles produced using OSA/MD, OSA/CS and pure OSA, the higher moisture contents observed may be due to the absence of IN, leading to a quick formation of the crust during the drying process, which hindered water release within the polymeric matrix (Fernandes et al., 2016). Moreover, MD tends to adsorb the water, and it is considered as a very hygroscopic material. Goula and Adamopoulos (2010) attributed the high water content of orange juice particles to high concentrations of MD.

Wettability represents the ability of a particle to interact with water molecules (C. Dima, Patrascu, Cantaragiu, Alexe, & Dima, 2016), and is related to the reconstitution process of particles. In this study, wettability was defined as the time required for the submergence of particles in water. The wettability time varied between 66s (OSA/IN nanoparticles) and 1036s (OSA/CS nanoparticles). The shorter time exhibited by the OSA/IN nanoparticles was most likely due to IN, which contains a large number of hydrophilic groups ( $-OH$ ), which enhance the ability of water molecules to adhere to

the particle surfaces. For this reason, the OSA/MD/IN and OSA/CS/IN treatments had lower wettability values compared to those using OSA/MD and OSA/CS. Lacerda et al. (2016) also observed that jussara pulp nanoparticles using IN showed a short wettability time (41s).

Solubility is used as a measurement of the stability of particles in water. The treatments studied showed significant differences ( $p < 0.05$ ) in their solubility ranging from 88.22% to 96.46%. This parameter is largely effected by the type of the carrier agent and the hydrophilic groups of the matrix structure (Yousefi & Emam-Djomeh, 2011). The OSA/MD/IN nanoparticles showed the higher water solubility at room temperature in comparison to the OSA/MD and OSA/IN ones ( $p < 0.05$ ), the reason seemed to be the formation of intermolecular hydrogen bonds between MD and IN. This was in agreement with the work (Meyer & Blaauwhoed, 2009) and they found that mixture of IN and water-binding materials, such as MD had significant effect on the solubility because of the formation of intermolecular hydrogen bonding. On the other hand, OSA/CS nanoparticles had the poor solubility because of the formation of electrostatic interactions between two opposite charged carbohydrates (Khong, Aarstad, Skjakbraek, Draget, & Varum, 2013). Moreover, the complex chemical structure of pure OSA, having hydrophobic regions, contributed to the decrease in the solubility of the particles observed (Botrel et al., 2017). For certain applications, high solubility is an essential property of particles being used as ingredients in food or beverage products. De Oliveira, Maia, De Figueiredo, and De Brito (2010) studied cashew juice using cashew gum and MD as wall materials with the solubility of 91.30%–96.40%,

indicating that OSA/MD/IN and OSA/CS/IN nanoparticles achieved the similar solubility with juice system.

The surface oil content is an index measuring the amount of un-encapsulated oil. The surface oil content of the nanoparticles produced using OSA, OSA/MD/IN, OSA/MD, OSA/CS/IN, OSA/CS and OSA/IN were 4.08%, 1.72%, 2.51%, 0.41%, 1.33% and 2.41%, respectively (**Table 3**). A larger amount of surface oil on the particles produced using pure OSA was observed, which may be due to the particles with wrinkled surfaces being able to capture oil droplets more easily than those with smoother surfaces. A similar high value of surface oil was found in a study on the microencapsulation of fish oil (6.90%) using modified starch as a carrier (Botrel et al., 2017). It was also noticed that the type of the wall material significantly influenced ( $p < 0.05$ ) the surface oil content of the particles, with the lowest value being observed for the OSA/CS/IN nanoparticles, followed by the OSA/MD/IN and OSA/CS particles. A low surface oil content means a high encapsulation efficiency (EE), which affects the quality of nanoparticles. The presence of IN as a third wall material showed a significant improvement ( $p < 0.05$ ) in this index value, probably because of the combination of these carbohydrates (OSA starch, MD/CS, IN) leading to the increased emulsification properties. Additionally, the type of carriers significantly influenced the formation of a crust during the spray drying by hindering or accelerating the spread of oil droplets on the surfaces of the particles (Aghbashlo, Mobli, Madadlou, & Rafiee, 2012). Thus, the combination of the carbohydrates studied in this work may have accelerated the formation of the crust and accordingly showed lower surface oil content

with high EE value. Moreover, the electrostatic interactions between the OSA starch and CS also contributed to the high quality of the OSA/CS/IN particles.

**Table 3.** Mean values and standard deviations for the moisture content, wettability, solubility, surface oil, encapsulation efficiency of the particles produced.

Treatment	Moisture content (%)	Wettability (s)	Solubility (%)	Surface oil ( g/100g nanopaticles)	Encapsulation efficiency (%)
OSA (control)	2.67 ± 0.14 <sup>a</sup>	374 ± 15 <sup>b</sup>	88.46 ± 0.57 <sup>c</sup>	4.08 ± 0.06 <sup>a</sup>	85.73 ± 0.21 <sup>d</sup>
OSA/MD	2.86 ± 0.12 <sup>a</sup>	208 ± 8 <sup>d</sup>	89.23 ± 0.58 <sup>b,c</sup>	2.51 ± 0.12 <sup>b</sup>	91.20 ± 0.42 <sup>c</sup>
OSA/CS	2.72 ± 0.14 <sup>a</sup>	1036 ± 32 <sup>a</sup>	88.22 ± 0.85 <sup>c</sup>	1.33 ± 0.08 <sup>c</sup>	95.34 ± 0.27 <sup>b</sup>
OSA/IN	1.27 ± 0.11 <sup>c</sup>	66 ± 8 <sup>e</sup>	90.96 ± 0.82 <sup>b,c</sup>	2.41 ± 0.04 <sup>b</sup>	91.56 ± 0.13 <sup>c</sup>
OSA/MD/IN	1.95 ± 0.10 <sup>b</sup>	81 ± 12 <sup>e</sup>	96.46 ± 2.23 <sup>a</sup>	1.72 ± 0.37 <sup>c</sup>	93.97 ± 1.31 <sup>b</sup>
OSA/CS/IN	1.73 ± 0.11 <sup>b</sup>	287 ± 11 <sup>c</sup>	93.18 ± 1.16 <sup>a,b</sup>	0.41 ± 0.07 <sup>d</sup>	98.57 ± 0.24 <sup>a</sup>

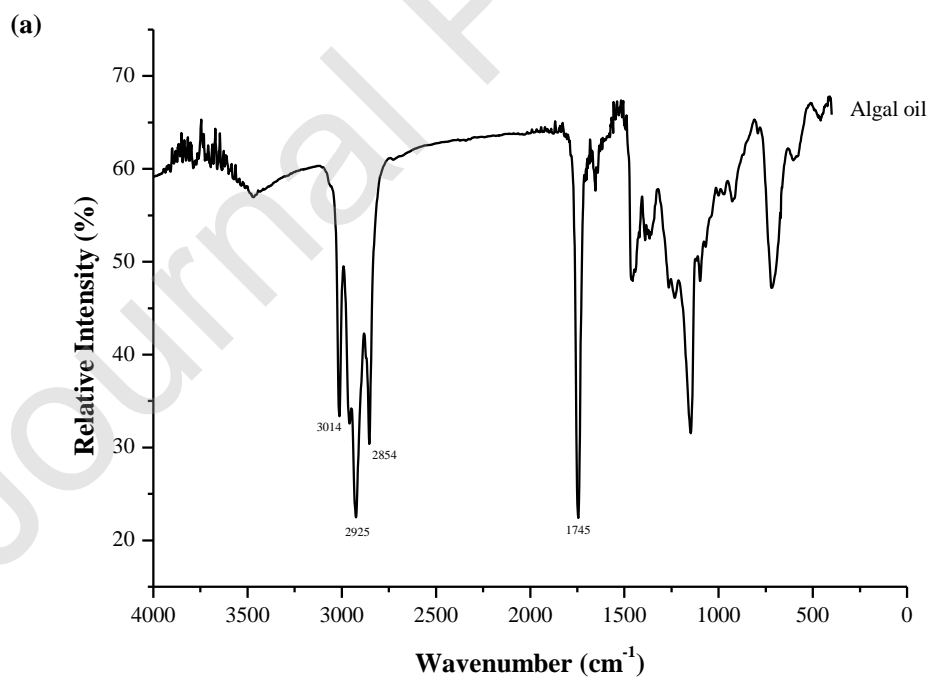
<sup>a,b,c,d,e</sup> Values with different letters at the same column differ significantly ( $p < 0.05$ ) by Duncan test. OSA (OSA starch), MD (maltodextrin), CS (chitosan), IN (inulin).

### 3.5. Fourier transform infrared spectroscopy of algal oil particles

FTIR analysis provide spectral absorption bands for encapsulated algal oil in the different materials studied, enabling identification of the presence of or changes to the functional groups and chemical bonds. **Figure 3a** shows the spectrum of pure algal oil. **Figures 3b, c** show that algal oil is encapsulated in the various wall materials, based on the appearance of absorption bands for C-H (2854, 2925, and 3014  $\text{cm}^{-1}$ ) and C=O (1745  $\text{cm}^{-1}$ ) bond stretching, which are typical representative bands of algal oil. Characteristic peaks at 1024, 1079, and 1153  $\text{cm}^{-1}$ , representative of C-O-C bond stretching of the anhydroglucose ring functional groups, are obtained for the pure OSA starch and all the particles, indicating a typical polysaccharide profile (Zhang et al.,

2011). Moreover, the band at  $1404\text{-}1419\text{ cm}^{-1}$  is associated with O-H bending, while the bound water in the wall materials resulted in the peaks at  $1641\text{ cm}^{-1}$ . Furthermore, the extremely broad band appearing at  $3386\text{-}3405\text{ cm}^{-1}$  is related to the stretching vibrations of free, intermolecular and intramolecular bound hydroxyl groups.

Compared to the other treatments, OSA/MD/IN, OSA/CS/IN nanoparticles show shifts in their hydroxyl group stretching vibration peaks from  $3405$  to  $3386\text{ cm}^{-1}$ , which are representative of improvements in hydrogen bonding among the encapsulating matrix. Furthermore, increases in the intensities of the C=O ( $1745\text{ cm}^{-1}$ ) band and O-H ( $3386\text{-}3405\text{ cm}^{-1}$ ) bands of the OSA/MD/IN and OSA/CS/IN treatments are observed, illustrating strong bonding interactions between the algal oil phase and the wall material system



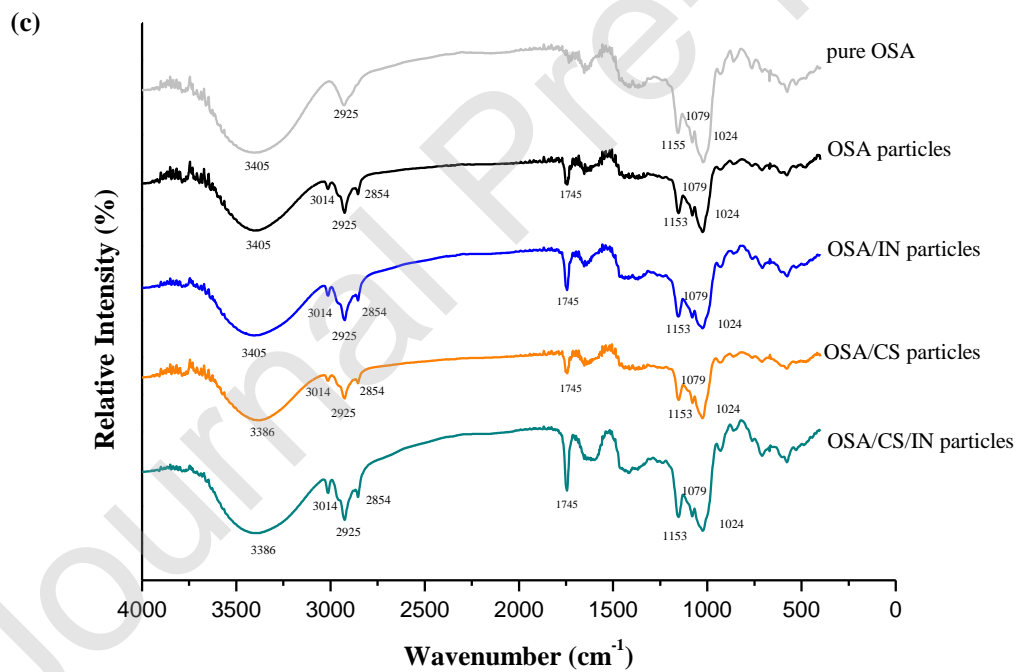
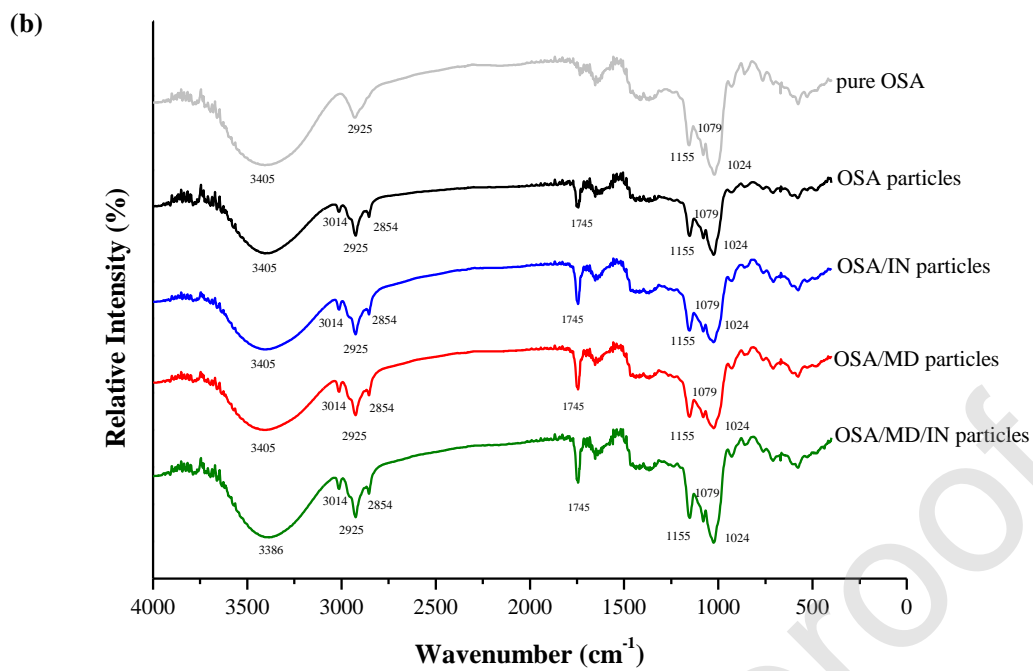


**Figure 3.** FTIR spectra of pure algal oil (a), FTIR spectra of pure OSA starch and the OSA, OSA/IN, OSA/MD, OSA/MD/IN nanoparticles (b). FTIR spectra of pure OSA starch and the OSA, OSA/IN, OSA/CS, OSA/CS/IN nanoparticles (c). OSA (OSA starch), MD (maltodextrin), CS (chitosan), IN (inulin).

### 3.6. Lipid oxidation of algal oil particles

In order to evaluate the lipid oxidation of the nanoparticles during storage, induction time (IT) was measured using the Rancimat accelerated oxidation method (**Figure 4**). This method has been accepted as an indirect indicator of lipid stability, with oils having IT values  $> 2$  h being considered stable (Interstandard, 2006). The method involves samples being treated under controlled conditions in which the oils are oxidized to short-chain volatile acids which increase the conductivity of distilled water. The longer it takes to increase the conductivity, the more stable the sample is (Di Giorgio, Salgado, & Mauri, 2019). The algal oil had an induction time of 0.67 h, implying low oxidative stability. The nanoparticles had IT values that were longer than that of the algal oil, indicating that the algal oil was microencapsulated in the nanoparticles.

In particular, the nanoparticles containing CS (OSA/CS/IN and OSA/CS) were the most stable samples, as they had the longest induction times. It turned out the electrostatic force between the OSA starch and CS contributed to the increased stability of the particles. Furthermore, the OSA/CS/IN nanoparticles had a higher oxidative stability (three times that of bulk oil) compared to that of the OSA/CS nanoparticles, which was most likely due to their lower surface oil content. In a study of Noello, Carvalho, Silva, and Hubinger (2016), chia oil had a 1.02 h IT, which was similar to the value found in the present study, and was also unstable. This may be because chia oil, like algal oil, contains high levels of polyunsaturated fatty acids. Moreover, Carvalho

et al. (2014) studied the lipid oxidation of particles of green coffee oil microencapsulated by lecithin-CS using the Rancimat method, and the addition of CS led to increased oxidative stability.

As shown in **Figure 4**, the IT value of the OSA/MD/IN nanoparticle was lower than that of the OSA/CS/IN and OSA/CS nanoparticles, but higher than that of OSA/MD and OSA/IN nanoparticles, which indicated that OSA/MD/IN nanoparticles had higher oxidative stability than that of the OSA/MD and OSA/IN particles. Probably for the reason that the combination of these carbohydrates (OSA starch, MD, and IN) contributing to its increased emulsification properties and high EE value.

It was also noted that the nanoparticles produced using pure OSA had the lowest oxidative stability. Besides their high surface oil content, the negative charges on the OSA starch may have had an impact on this result. As Noello, Carvalho, Silva, and Hubinger (2016) pointed out, particles produced using chia oil and WPC/pectin were more susceptible to oxidation compared to particles produced using chia oil and pure WPC. The lower stability of the chia oil/WPC/pectin particles was related to the presence of pectin's negative charge, which accelerated the adsorption of  $\text{Fe}^{2+}$  ions on the lipid surface and promoted lipid oxidation. This could also explain why the OSA/CS/IN nanoparticles, which had a positive charge on their outer layers, had the highest oxidative stability.

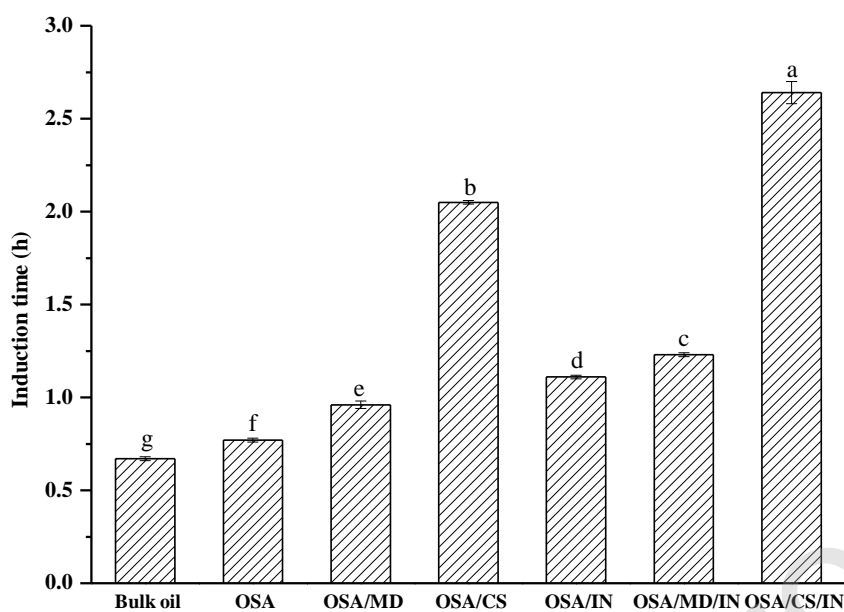


**Figure 4.** Induction time obtained by the Rancimat method for nanoparticles produced with the different wall material systems and bulk algal oil as control. <sup>a,b,c,d,e,f,g</sup> Values with different letters at the same column differ significantly ( $p < 0.05$ ) by Duncan test. OSA (OSA starch), MD (maltodextrin), CS (chitosan), IN (inulin).

### 3.7. Moisture adsorption isotherm of algal oil particles

The presence of water is crucial to food storage, as the moisture content and moisture absorption of food materials during storage largely determines food product quality (Shivhare, 2006). A plot of these values (moisture content versus moisture adsorption) represents a moisture absorption isotherm, which is a typical and practical method of revealing the hygroscopic properties of food materials. Furthermore, it is a convenient way of predicting the stability of food products enabling better selection of

ingredients or suitable storage conditions in the food industry (Al-Muhtaseb, Mcminn, & Magee, 2002).

**Table 4** presents the estimated values of the coefficients and statistical parameters that were used to judge the suitability of the models (GAB, BET, Halsey, Henderson, Oswin, and Smith) to determine the moisture adsorption behavior of the algal oil nanoparticles of three different emulsions (OSA nanoparticles were used as a control). As shown in **Figure 5a**, the moisture absorption of all the three treatments showed noticeable increase when the water activity exceeded 0.75. For OSA/CS/IN and pure OSA powders, their equilibrium water contents reached 11.50 and 7.19 g/100 g of dry basis, respectively, at  $a_w$  0.75, indicating the higher hygroscopicity of the OSA/CS/IN nanoparticles. The equilibrium water content value of the OSA/CS/IN nanoparticles was also lower than the minimum equilibrium water content of fish oil-containing particles produced using pure modified starch (12.50 g/100 g;  $a_w = 0.75$ ) studied by Botrel et al. (2017). The reason for this seems to be that the addition of IN as a drying aid agent has a significant effect on the water adsorption ability of the algal oil particles. According to Botrel and Souza (2016), the equilibrium water contents of treatments containing IN were obviously lower compared to those of pure araticum powder at a given  $a_w$ . Additionally, the isotherm curves for all three emulsions were type II (sigmoidal), which is convex upwards at low  $a_w$ , reflective of strong interactions between adsorbate and adsorbent (Younce, 2010).

The GAB, BET, Halsey, Henderson, Oswin and Smith models were compared in

order to establish the best model to describe the isotherm behavior of the algal oil nanoparticles. The GAB model was selected as the best model because it possessed the lowest relative mean error (E) and highest adjusted R-squared (Adj.  $R^2$ ) values. Fernandes et al. (2014), who studied the microencapsulation of rosemary essential oil using a starch/IN system, also found that the GAB model presented a good fit for their data. By applying this model, the monolayer moisture content ( $X_m$ ), which is a useful parameter for food quality and food product storage, was determined to establish appropriate storage conditions for the particles. It was discovered that the  $X_m$  value of the OSA/CS/IN powder was higher than that of the other powders, indicating that a greater amount of water strongly adsorbed to specific sites on the OSA/CS/IN nanoparticle surfaces.

The  $X_m$  is an essential moisture threshold where dried ingredients are more stable. The OSA/CS/IN powder had consistently high water absorption values across the entire  $a_w$  range. However, no physical change in the appearance of the OSA/CS/IN nanoparticles was observed. Additionally, this powder was the only one to remain in a relatively stable state for the series of water activities studied, which was probably due to its high threshold  $X_m$  value. In contrast, the OSA and OSA/MD/IN nanoparticles did experience phase changes, from glassy to rubbery states, which were attributed to the room temperature being higher than the glass transition temperatures of the powders at  $a_w$  0.98. Therefore, use of an OSA/CS/IN system as a new approach for algal oil microencapsulation works well, as it can remain relatively stable even at high levels of humidity.

**Table 4.** Estimated values of the coefficients and statistical parameters for the studied models: GAB, BET, Halsey, Henderson, Oswin and Smith.

Model and equation		OSA	OSA/MD/IN	OSA/CS/IN
GAB $X_{eq} = \frac{X_m C K a_w}{(1 - K a_w)(1 - K a_w + C K a_w)}$	$X_m$	0.023	0.034	0.042
	C	22.736	68.601	53.665
	K	0.895	0.869	0.858
	E(%)	5.511	4.082	4.100
	Adj. R <sup>2</sup>	0.995	0.997	0.997
BET $X_{eq} = \frac{X_m C a_w}{1 - a_w} \left[ \frac{1 - (n + 1)(a_w)^n + n(a_w)^{n+1}}{1 - (1 - C)a_w - C(a_w)^{n+1}} \right]$	$X_m$	15.044	35.154	51.812
	C	0.001	0.001	0.001
	n	4.587	3.065	2.639
	E(%)	39.799	37.628	34.691
	Adj. R <sup>2</sup>	0.914	0.877	0.878
Halsey $X_{eq} = \left( \frac{a}{\ln a_w} \right)^{1/b}$	a	0.000	0.000	-0.001
	b	2.397	2.733	2.835
	E(%)	17.311	12.123	13.094
	Adj. R <sup>2</sup>	0.981	0.981	0.984
Henderson $X_{eq} = \left[ \frac{\ln(1 - a_w)}{-a} \right]^{1/b}$	a	27.327	30.983	27.736
	b	1.152	1.376	1.446
	E(%)	16.963	14.746	12.440
	Adj. R <sup>2</sup>	0.987	0.981	0.984
Oswin $X_{eq} = a \left[ \frac{a_w}{(1 - a_w)} \right]^b$	a	0.045	0.065	0.080
	b	0.374	0.326	0.313
	E(%)	8.737	5.679	6.067
	Adj. R <sup>2</sup>	0.994	0.993	0.992
Smith $X_{eq} = a + b \log(1 - a_w)$	a	0.009	0.021	0.027
	b	-0.105	-0.124	-0.144
	E(%)	9.033	7.628	6.504
	Adj. R <sup>2</sup>	0.992	0.981	0.976

$X_{eq}$ : equilibrium moisture content ( $\text{g} \cdot \text{g}^{-1}$  dry powder);  $X_m$ : monolayer moisture content ( $\text{g} \cdot \text{g}^{-1}$  dry powder);

C, K: model constants related to the monolayer and monolayer properties;  $a_w$ : water activity; a, b: model parameters; E: relative mean error; Adj. R<sup>2</sup>: adjusted R-square value; OSA (OSA starch), MD

(maltodextrin), CS (chitosan), IN (inulin).

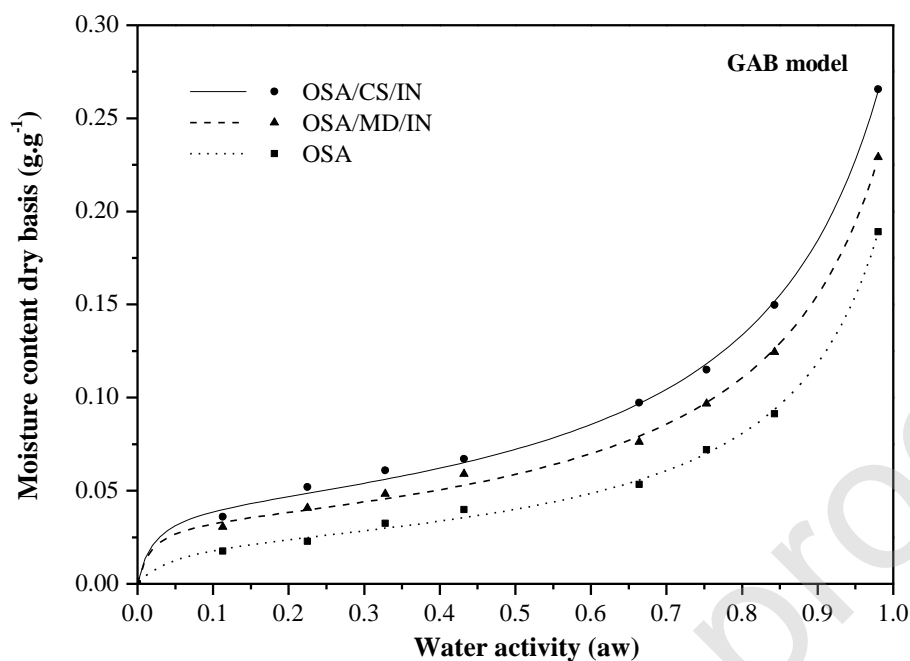


**Figure 5.** Moisture adsorption isotherms adjusted by the GAB model of the nanoparticles produced using the different wall material systems in the water activity range of 0.11-0.98. OSA (OSA starch), MD (maltodextrin), CS (chitosan), IN (inulin).

### 3.8 Thermogravimetric analysis of algal oil particles

Thermogravimetric analysis (TGA) involves the measurement of changes in sample weight with temperature and was used to assess the thermal stability of the treatments. The first derivative of a TG curve indicates the intensity of the weight loss due to decomposition or combustion at a certain temperature. This derivative thermogravimetric (dTG) curve clearly reflected the initial reaction temperature, the temperature of the maximum weight loss rate, and the final reaction temperature as shown in **Figure 6**.

All of the particles containing algal oil had four weight loss stages. (1) At temperatures  $\leq 120$  °C the weight loss was related to a loss of moisture (3.60%) by the particles, with the low value observed indicating low moisture content. (2) At temperatures  $> 120$  °C the weight loss was related to reactions of the wall materials (IN, MD/CS, and OSA starch) (Seyed Fakhreddin, Mojgan, Masoud, & Farhid, 2013). A 5.20% (95.76 - 90.56%) mass loss occurred in the range of 200–250 °C for IN. (3) In the range of 250–360 °C, significant peaks were observed in the dTG curves. The weight loss of the samples was 51.50% (90.56 - 39.06%), which was due to the combined decomposition of OSA starch, MD, or CS at the same temperature. (4) In the range of 360–500 °C, the samples lost 31.11% (39.06 - 7.95%) in weight, mainly because the internal algal oil began to decompose.

Comparing the pure wall materials to algal oil, it was observed that the temperature of the maximum weight loss rate of algal oil shifted from 378 °C to 400 °C, as the algal oil was encapsulated by the wall materials which provided a layer of protection. Furthermore, the mass loss of the OSA/MD/IN and OSA/CS/IN particles occurred at a temperature over 200 °C, showing the superior thermal stability of the products.

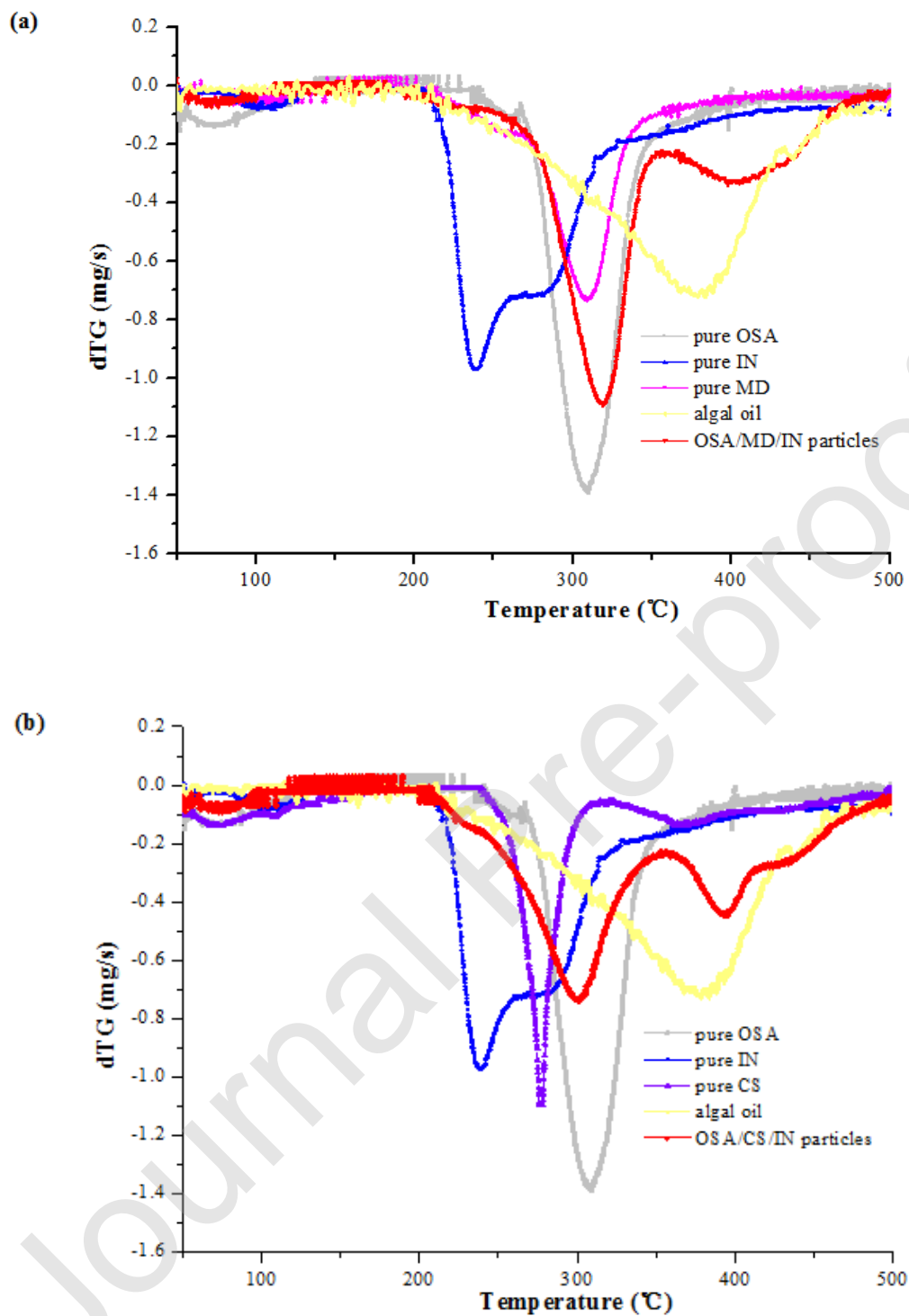


**Figure 6.** dTG curves: raw materials and nanoparticles containing algal oil produced with OSA/MD/IN (a) and OSA/CS/IN (b). OSA (OSA starch), MD (maltodextrin), CS (chitosan), IN (inulin).

#### **4. Conclusion**

This study investigated the potential use of prebiotic biopolymers in algal oil nanocapsules. Based on the results of this study, the OSA/CS/IN encapsulation system presented the most desirable properties. The OSA/CS/IN particles showed no cracks, and fewer dents, compared to the pure OSA and OSA/MD/IN particles. Furthermore, the OSA/CS/IN particles exhibited superior solubility and physicochemical stability. Specifically, the OSA/CS/IN nanoparticles had a more prominent in solubility (96.46%) than the OSA/CS particles because of the formation of intermolecular hydrogen bonds, which was supported by FTIR analysis. Additionally, as there were electrostatic interactions between the CS and OSA starch, the OSA/CS/IN particles performed the highest encapsulation efficiency (98.57%) and oxidative stability (three times that of bulk oil). Furthermore, the OSA/CS/IN nanoparticles did not undergo phase transition at  $a_w$  0.98, maintaining stability even at high humidity. Thermogravimetric analysis further demonstrated that hybrid encapsulation could enhance the thermal stability of algal oil. In conclusion, the search for new approaches of encapsulation is urgent in the food industry and OSA/CS/IN, as a prebiotic carbohydrates system, shows great potential and feasibility.

#### **Conflict of interest**

The authors declare no conflict of interest.

#### **Acknowledgements**

This work was supported by the Natural Science Foundation of China (31871840) and

National Key R&D Program of China (2016YFD0401404).

## References

- Aghbashlo, M., Mobli, H., Madadlou, A., & Rafiee, S. (2012). The correlation of wall material composition with flow characteristics and encapsulation behavior of fish oil emulsion. *Food Research International*, 49(1), 379-388.
- Akhavan, S., Assadpour, E., Katouzian, I., & Jafari, S. M. (2018). Lipid nano scale cargos for the protection and delivery of food bioactive ingredients and nutraceuticals. *Trends in Food Science & Technology*, 74.
- Al-Muhtaseb, A. H., Mcminn, W. A. M., & Magee, T. R. A. (2002). Moisture Sorption Isotherm Characteristics of Food Products: A Review. *Food & Bioproducts Processing*, 80(2), 118-128.
- Botrel, D. A., Borges, S. V., Antoniassi, R., Faria-Machado, A. F. D., Feitosa, J. P. D. A., & Paula, R. C. M. D. (2017). Application of cashew tree gum on the production and stability of spray-dried fish oil. *Food Chemistry*, 221, 1522.
- Botrel, D. A., Borges, S. V., Yoshida, M. I., de Andrade Feitosa, J. P., de Barros Fernandes, R. V., de Souza, H. J. B., & de Paula, R. C. M. (2017). Properties of spray-dried fish oil with different carbohydrates as carriers. *Journal of food science and technology*, 54(13), 4181-4188.
- Botrel, D. A., de Barros Fernandes, R. V., Borges, S. V., & Yoshida, M. I. (2014). Influence of wall matrix systems on the properties of spray-dried microparticles containing fish oil. *Food Research International*, 62, 344-352.
- Botrel, D. A., & Souza, H. J. B. D. (2016). Application of inulin in thin-layer drying process of araticum (*Annona crassiflora*) pulp. *LWT - Food Science and Technology*, 69, 32-39.
- Bule, M. V., Singhal, R. S., & Kennedy, J. F. (2010). Microencapsulation of ubiquinone-10 in carbohydrate matrices for improved stability. *Carbohydrate Polymers*, 82(4), 1290-1296.
- Cano-Chauca, M., Stringheta, P. C., Ramos, A. M., & Cal-Vidal, J. (2005). Effect of the carriers on the microstructure of mango powder obtained by spray drying and its functional characterization. *Innovative Food Science & Emerging Technologies*, 6(4), 420-428.
- Carneiro, H. C. F., Tonon, R. V., Grosso, C. R. F., & Hubinger, M. D. (2013). Encapsulation efficiency and oxidative stability of flaxseed oil microencapsulated by spray drying using different combinations of wall materials. *Journal of Food Engineering*, 115, 443-451.
- Carvalho, A., Silva, V., & Hubinger, M. (2014). Microencapsulation by spray drying of emulsified green coffee oil with two-layered membranes. *Food Research International*, 61, 236-245.
- Che, H., Li, Q., Zhang, T., Wang, D., & Wang, Y. (2018). The effects of astaxanthin and docosahexaenoic acid-acylated astaxanthin on Alzheimer's disease in APP/PS1 double transgenic mice. *Journal of Agricultural and Food Chemistry*, 66(19), acs.jafc.8b00988.
- Cho, S. S., & Samuel, P. (2009). *Fiber ingredients: food applications and health benefits*: CRC press.
- De Oliveira, M. A., Maia, G. A., De Figueiredo, R. W., & De Brito, E. S. (2010). Addition of cashew tree gum to maltodextrin-based carriers for spray drying of cashew apple juice. *International Journal of Food Science & Technology*, 44(3), 641-645.
- Di Giorgio, L., Salgado, P. R., & Mauri, A. N. (2019). Encapsulation of fish oil in soybean protein

- particles by emulsification and spray drying. *Food Hydrocolloids*, 87, 891-901.
- Dima, C., Patrascu, L., Cantaragiu, A., Alexe, P., & Dima, S. (2016). The kinetics of the swelling process and the release mechanisms of *Coriandrum sativum* L. essential oil from chitosan/alginate/inulin microcapsules. *Food Chem*, 195, 39-48.
- Dima, C., Pătrașcu, L., Cantaragiu, A., Alexe, P., & Dima, Ș. (2015). The kinetics of the swelling process and the release mechanisms of *Coriandrum sativum* L. essential oil from chitosan/alginate/inulin microcapsules. *Food Chemistry*, 195(2), 39-48.
- Encina, C., Vergara, C., Giménez, B., Oyarzún-Ampuero, F., & Robert, P. (2016). Conventional spray-drying and future trends for the microencapsulation of fish oil. *Trends in Food Science & Technology*, 56, 46-60.
- Fernandes, R. V., Borges, S. V., & Botrel, D. A. (2014). Gum arabic/starch/maltodextrin/inulin as wall materials on the microencapsulation of rosemary essential oil. *Carbohydr Polym*, 101, 524-532.
- Fernandes, R. V. B., Botrel, D. A., Silva, E. K., Borges, S. V., Oliveira, C. R., Yoshida, M. I., de Paula, R. C. M. (2016). Cashew gum and inulin: New alternative for ginger essential oil microencapsulation. *Carbohydr Polym*, 153, 133-142.
- Frascareli, E. C., Silva, V. M., Tonon, R. V., & Hubinger, M. D. (2012). Effect of process conditions on the microencapsulation of coffee oil by spray drying. *Food & Bioproducts Processing*, 90(3), 413-424.
- Fuchs, M., Turchiuli, C., Bohin, M., Cuvelier, M. E., Ordonnaud, C., Peyrat-Maillard, M. N., & Dumoulin, E. (2006). Encapsulation of oil in powder using spray drying and fluidised bed agglomeration. *Journal of Food Engineering*, 75(1), 27-35.
- García, E., Gutiérrez, S., Nolasco, H., Carreón, L., & Arjona, O. (2006). Lipid composition of shark liver oil: effects of emulsifying and microencapsulation processes. *European Food Research & Technology*, 222(5-6), 697-701.
- Garcia, L. C., Tonon, R. V., & Hubinger, M. D. (2012). Effect of Homogenization Pressure and Oil Load on the Emulsion Properties and the Oil Retention of Microencapsulated Basil Essential Oil (*Ocimum basilicum* L.). *Drying Technology*, 30(13), 1413-1421.
- Giorgio, L. D., Salgado, P. R., & Mauri, A. N. (2019). Encapsulation of fish oil in soybean protein particles by emulsification and spray drying. *Food Hydrocolloids*, 87, 891-901.
- Goula, A. M., & Adamopoulos, K. G. (2010). A new technique for spray drying orange juice concentrate. *Innovative Food Science & Emerging Technologies*, 11(2), 342-351.
- Hategekimana, J., Masamba, K. G., Ma, J., & Zhong, F. (2015). Encapsulation of vitamin E: effect of physicochemical properties of wall material on retention and stability. *Carbohydr Polym*, 124, 172-179.
- He, H., Hong, Y., Gu, Z., Liu, G., Cheng, L., & Li, Z. (2016). Improved stability and controlled release of CLA with spray-dried microcapsules of OSA-modified starch and xanthan gum. *Carbohydr Polym*, 147, 243-250.
- Hwang, J. K., & Shin, H. H. (2000). Rheological properties of chitosan solutions. *Korea-Australia Rheology Journal*, 12(3/4), 175-179.
- Interstandard. (2006). Animal and vegetable fats and oils. Determination of oxidative stability (accelerated oxidation test). *Iso International Standard*.
- Jafari, S. M., Assadpoor, E., Bhandari, B., He, Y., Jafari, S. M., & Assadpoor, E. (2008). Nano-particle encapsulation of fish oil by spray drying. *Food Research International*, 41(2), 172-

183.

- Jafari, S. M., Assadpoor, E., He, Y., & Bhandari, B. (2008). Encapsulation Efficiency of Food Flavours and Oils during Spray Drying. *Drying Technology*, 26(7), 816-835.
- Khong, T. T., Aarstad, O. A., Skjakbraek, G., Draget, K. I., & Varum, K. M. (2013). Gelling Concept Combining Chitosan and Alginate-Proof of Principle. *Biomacromolecules*, 14(8), 2765-2771.
- Klinkesorn, U., Decke, E. A., & McClements, D. J. (2006). Characterization of spray-dried tuna oil emulsified in two-layered interfacial membranes prepared using electrostatic layer-by-layer deposition. *Food Research International*, 39(4), 449-457.
- Lacerda, E. C. Q., Calado, V. M. A., Monteiro, M., Finotelli, P. V., Torres, A. G., & Perrone, D. (2016). Starch, inulin and maltodextrin as encapsulating agents affect the quality and stability of jussara pulp microparticles. *Carbohydr Polym*, 151, 500-510.
- Menin, A., Zaroni, F., Vakarelova, M., Chignola, R., Donà, G., Rizzi, C., . . . Zoccatelli, G. (2018). Effects of microencapsulation by ionic gelation on the oxidative stability of flaxseed oil. *Food Chemistry*, 269, 293-299.
- Mensink, M. A., Frijlink, H. W., van der Voort Maarschalk, K., & Hinrichs, W. L. (2015). Inulin, a flexible oligosaccharide I: Review of its physicochemical characteristics. *Carbohydrate Polymers*, 130, 405-419.
- Meyer, D., & Blaauwloed, J.-P. (2009). Inulin. In *Handbook of hydrocolloids* (pp. 829-848): Elsevier
- Mirhosseini, H., Tan, C. P., Hamid, N. S. A., & Yusof, S. (2008). Optimization of the contents of Arabic gum, xanthan gum and orange oil affecting turbidity, average particle size, polydispersity index and density in orange beverage emulsion. *Food Hydrocolloids*, 22(7), 1212-1223.
- Noello, C., Carvalho, A. G. S., Silva, V. M., & Hubinger, M. D. (2016). Spray dried microparticles of chia oil using emulsion stabilized by whey protein concentrate and pectin by electrostatic deposition. *Food Research International*, 89(Pt 1), 549-557.
- Nsofor, L. M., & Osuji, C. M. (1997). Stability, rheology and chemical properties of soymilk concentrates developed from sprouted soybeans. *Journal of Food Science and Technology*, 34, 33-40.
- Nunes, G. L., de Araújo Etchepare, M., Cichoski, A. J., Zepka, L. Q., Lopes, E. J., Barin, J. S., de Menezes, C. R. (2018). Inulin, hi-maize, and trehalose as thermal protectants for increasing viability of *Lactobacillus acidophilus* encapsulated by spray drying. *LWT-Food Science and Technology*, 89, 128-133.
- Ortea, I., Gonzalez-Fernandez, M. J., Ramos-Bueno, R. P., & Guerrero, J. L. G. (2018). Proteomics Study Reveals That Docosahexaenoic and Arachidonic Acids Exert Different In Vitro Anticancer Activities in Colorectal Cancer Cells. *Journal of Agricultural & Food Chemistry*, 66(24), 6003-6012.
- Otalora, M. C., Carriazo, J. G., Iturriaga, L., Nazareno, M. A., & Osorio, C. (2015). Microencapsulation of betalains obtained from cactus fruit (*Opuntia ficus-indica*) by spray drying using cactus cladode mucilage and maltodextrin as encapsulating agents. *Food Chem*, 187, 174-181.
- Reineccius, G. A. (2004). The Spray Drying of Food Flavors. *Drying Technology*, 22(6), 1289-1324.
- Seyed Fakhreddin, H., Mojgan, Z., Masoud, R., & Farhid, F. (2013). Two-step method for

- encapsulation of oregano essential oil in chitosan nanoparticles: preparation, characterization and in vitro release study. *Carbohydr Polym*, 95(1), 50-56.
- Shivhare, U. S. (2006). Models for Sorption Isotherms for Foods: A Review. *Drying Technology*, 24(8), 917-930.
- Silva, E. K., Zobot, G. L., Cazarin, C. B. B., Jr, M. R. M., & Meireles, M. A. A. (2016). Biopolymer-prebiotic carbohydrate blends and their effects on the retention of bioactive compounds and maintenance of antioxidant activity. *Carbohydrate Polymers*, 144, 149-158.
- Sun-Waterhouse, D. (2011). The development of fruit - based functional foods targeting the health and wellness market: a review. *International Journal of Food Science & Technology*, 46(5), 899-920.
- Utai, K., Pairat, S., Pavinee, C., D Julian, M., & Decker, E. A. (2005). Stability of spray-dried tuna oil emulsions encapsulated with two-layered interfacial membranes. *J Agric Food Chem*, 53(21), 8365-8371.
- Wang, Q., Jiang, J., & Xiong, Y. L. (2018). High pressure homogenization combined with pH shift treatment: A process to produce physically and oxidatively stable hemp milk. *Food Res Int*, 106, 487-494.
- Younce, F. (2010). ENGINEERING PROPERTIES OF FOODS. *Journal of Food Processing & Preservation*, 30(2), 246-246.
- Yousefi, S., & Emam-Djomeh, Z. (2011). Effect of carrier type and spray drying on the physicochemical properties of powdered and reconstituted pomegranate juice (*Punica Granatum L.*). *Journal of Food Science & Technology*, 48(6), 677-684.
- Zhang, B., Huang, Q., Luo, F. X., Fu, X., Jiang, H., & Jane, J. L. (2011). Effects of octenylsuccinylation on the structure and properties of high-amylose maize starch. *Carbohydrate Polymers*, 84(4), 1276-1281.